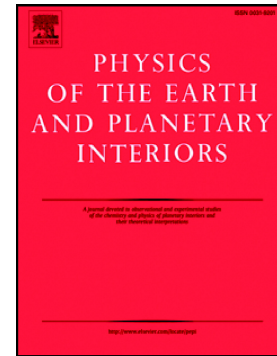


Dating a medieval pottery workshop of the city of Burgos (Spain):
Archaeomagnetic and archaeological evidences

Ángela Herrejón-Lagunilla, Juan José Villalaín, Ángel Carrancho,
Carmen Alonso-Fernández, Javier Jiménez-Echevarría, Francisco
Javier Pavón-Carrasco



PII: S0031-9201(21)00081-9

DOI: <https://doi.org/10.1016/j.pepi.2021.106723>

Reference: PEPI 106723

To appear in: *Physics of the Earth and Planetary Interiors*

Received date: 29 September 2020

Revised date: 25 April 2021

Accepted date: 28 April 2021

Please cite this article as: Á. Herrejón-Lagunilla, J.J. Villalaín, Á. Carrancho, et al., Dating a medieval pottery workshop of the city of Burgos (Spain): Archaeomagnetic and archaeological evidences, *Physics of the Earth and Planetary Interiors* (2021), <https://doi.org/10.1016/j.pepi.2021.106723>

This is a PDF file of an article that has undergone enhancements after acceptance, such as the addition of a cover page and metadata, and formatting for readability, but it is not yet the definitive version of record. This version will undergo additional copyediting, typesetting and review before it is published in its final form, but we are providing this version to give early visibility of the article. Please note that, during the production process, errors may be discovered which could affect the content, and all legal disclaimers that apply to the journal pertain.

Dating a medieval pottery workshop of the city of Burgos (Spain): archaeomagnetic and archaeological evidences

Ángela Herrejón-Lagunilla^{1,*} angelaherregonlagunilla@gmail.com, Juan José Villalain¹,
Ángel Carrancho², Carmen Alonso-Fernández³, Javier Jiménez-Echevarría³, Francisco
Javier Pavón-Carrasco⁴.

¹Dpto. de Física. Universidad de Burgos. Escuela Politécnica Superior (Campus Río Vena),
Avda. Cantabria s/n, 09006. Burgos (Spain). angelaherregonlagunilla@gmail.com, villa@ubu.es

²Área de Prehistoria, Departamento de Historia, Geografía y Comunicación, Universidad de
Burgos. Edificio I+D+I, Plaza Misael Bañuelos s/n, Burgos (Spain). acarrancho@ubu.es

³Cronos S.C. Arqueología y Patrimonio. C/ Aparicio y Ruiz 16, 4º Dcha, 09003. Burgos
(Spain). ca@cronossc.es; jj@cronossc.es

⁴Dpto. de Física de la Tierra y Astrofísica. Facultad de Ciencias Físicas. Universidad
Complutense, Madrid (Spain). fjpavon@ccm.es

*Corresponding author.

ABSTRACT

Here we report a detailed archaeomagnetic and rock-magnetic study of a pottery kiln from Burgos (Spain) to reconstruct its burning conditions and date its last use and abandonment age. During the course of a rescue archaeological excavation carried out in 2015 in the center of Burgos city, a medieval pottery workshop was discovered. Two well-preserved kilns appeared and archaeomagnetic analyses were performed on one of them. In addition to a large amount of pottery remains, some numismatic and documental evidences provided a general chronological estimation, but the abandonment age of the workshop remains unknown. On the basis of the existing archaeological information we carried out an archaeomagnetic study in order to date its last use. 69 archaeomagnetic samples were collected from the combustion chamber and the

kiln's fire tunnel. Stepwise alternating field and thermal demagnetization of the natural remanent magnetization (NRM) were carried out to retrieve the mean direction. Additional experiments consisted in the acquisition of isothermal remanence (IRM), low-field magnetic susceptibility and its anisotropy as well as thermomagnetic curves. Despite the high temperatures expected in the combustion chamber, it appeared that the bricks' samples from the fire tunnel exhibit the most successful directional results. Magnetite and variable contributions of hematite are the main ferromagnetic minerals observed in the thermomagnetic curves. The type of lithology studied, its previous magnetic history and their location in the kiln strongly condition the observed directional and rock-magnetic results. Additionally, AMS data revealed the manufacturing fabric of the fire tunnel's bricks, showing moderately high anisotropy degrees, but not enough to cast doubts on the directional NRM record. In order to test the reproducibility of the dating results, archaeomagnetic dating was carried out using different geomagnetic field models and the Iberian secular variation curve. The small differences observed in the dating results are mainly due to the density and type of input data of these records. The combination of the archaeomagnetic analyses with the archaeological and documental suggests that last kiln's usage took place during the first half of the XVIth century AD. Overall, this paper illustrates how the combination of archaeological data and archaeomagnetic analyses may improve our understanding about the manufacturing processes, use and age of abandonment of archaeological combustion structures.

KEYWORDS: Archaeomagnetic dating; rock magnetism; burnt materials; kiln

1. INTRODUCTION

During construction and remodeling works in the cities, unexpected findings may often be discovered. During the course of a rescue archaeological excavation carried out in 2015 in Burgos city (north-central Spain), the Vega's pottery workshop was unearthed. The discovery took place during the construction of a building in San Ignacio de Loyola Street, next to the

church and old convent of Nuestra Señora de La Merced (**Fig. 1a-b**). It was located outside the medieval walls of the city in a poorly urbanized area sited in the historic Vega suburbs (Crespo Redondo, 2007). Due to the later urban development in the area because of the interest of the emergent bourgeoisie and outside-walls monasteries (like La Merced), pottery production became a disturbing activity in this area. Therefore, the workshop was closed and pottery production was moved to another location.

Fig. 1. (a) Map of the Iberian Peninsula with the location of Burgos and (b) schematic plane of the central area of Burgos showing the location of the pottery workshop (yellow star).

Stratigraphic data and the typology of the recovered pottery remains suggest that the workshop was operative between the last quarter of XIVth century and the first decades of the XVIth century AD (**Supplementary Materials 1 and 2**). This makes this workshop one of the few pottery production centers systematically studied in the regional context for this period so far. Moreover, it exhibits some singularities (not only at regional scale, but also for all the Iberian Peninsula) like the production of Jewish pieces (bowls and plates with shapes A and B in **Supplementary Material 1**) with Hebrew signs. However, it is not easy to determine the final closure of the workshop, since documental and archaeological evidences do not allow to accurately establish its abandonment's age. Archaeomagnetic dating is probably the most suitable tool for this purpose (i.e.: Carrancho *et al.* 2017; García-Redondo *et al.* 2019, 2020) but still far from being routinely applied in many archaeological research projects. Thus, here we report a detailed study combining stratigraphic data, pottery analyses and the archaeomagnetic dating of one of the kilns of the Vega's workshop in order to constrain the date of its final closure. It is important since this moment corresponds to the evolution of the first Renaissance societies in the region, whose material culture is not well-known yet. We also point out problems concerning the type of materials and lithology used in this type of structures and their

suitability for archaeomagnetic purposes. All this information will be valuable not only to improve our knowledge about the recent past in the region but also aiding to improve the dating technique when studying similar combustion structures.

2. MATERIALS AND METHODS

2.1. Vega's workshop and Western kiln features

The excavations in the pottery workshop of Vega uncovered two kilns (western and eastern). The possibility of carrying out an archaeomagnetic study here arose when only the western kiln remained to be excavated. The western kiln (studied here) presents two main parts: the combustion chamber and a fire tunnel (**Fig. 2**). The combustion chamber has a circular shape with an inner diameter of 2,3 m. Its lower part consists of a bowl-shaped clayey basis. Its height reaches up to 45 cm approximately. One or two lines of sandstone masonry blocks settle above this. There are two trapezoidal pillars of up to 50 cm of width, attached to the inner wall of the combustion chamber and located close to the East and the West respectively. They were used to support the grill (perforated surface on which the objects to be heated are placed), but this raised oven floor is not preserved.

Fig. 2. General view of the studied kiln, showing the approximated location of sampled areas (inner diameter of combustion chamber = 2.3 m).

The fire tunnel is located at the North-Northwest of the combustion chamber and has a Northwest-Southeast orientation (**Fig. 2**). It is wider in the inner part than the outer part (100 cm of width vs. 55 cm respectively, although a masonry sandstone block in the eastern wall of the fire tunnel narrows the passage to 40 cm in the outer extreme). The fire tunnel reaches a length of 1,3 m. The foundation of this part of the kiln consists of sandstone masonry above which several rows of bricks were placed and fixed with clay. The dimensions of the bricks are

36 x 16 x 3 cm. In the east wall of the fire tunnel, there are 13 rows of bricks preserved, reaching 53 cm of height (70 cm considering the foundation).

The recovery of several types of archaeological materials, such as a big amount of pottery pieces (**Supplementary Materials 1**), allowed to propose ten chronological phases for the archaeological sequence of Vega's site, ranging from XIIth century AD up to the present times (**Supplementary Materials 2**). In spite of this, the chronological assessment of the closure of the workshop is difficult to be approached. It seems that the activity of western kiln stopped before the abandonment of the eastern one. After closure of western kiln, it was filled with different materials, including a coin from the epoch of the Catholic Monarchs (*blanca*). Catholic Monarchs governed between 1469 and 1504 AD, but there is not any precise information about the moment of their reign in which this piece was coined. Moreover, it is not known how much time elapsed between the abandonment of the structure and its filling. Anyway, it is sure that filling happened necessarily after its abandonment. Since the coin was minted in some moment between 1469 and 1504 AD, the filling had to take place after 1469. This date can be used as a *terminus post quem* for the filling. Apart from this, documental evidence (Archivo Municipal de Purgos, HI-3612) reveals the existence of several houses in the area in 1545 AD. Taking into account this source, the workshop had stopped working completely by 1545 AD. This data can be used as the *terminus ante quem*. Considering these issues, it was decided to carry out archaeomagnetic analyses on the western kiln. This procedure can help to assess the date of its last use with more precision.

2.2. Sampling

With the purpose of carrying out an archaeomagnetic dating, 69 oriented samples were extracted from different parts of the oven: 32 of them come from the bricks of the fire tunnel (East and West profiles in **Fig. 2**, also called PE and PW respectively) and the 37 remaining ones correspond to limestones, quartzite and sandstones from the combustion chamber (areas PV3 to PV9 and PB, **Fig. 2**) and the basis of the area where the combustion chamber and fire

tunnel adjoin (below the bricks' rows level; areas PV1 and PV2, **Fig. 2**). Hereinafter, all those materials which are not strictly fire tunnel's bricks (PV1-9 and PB) will be identified as "other materials" or "non-brick materials", in reference to limestones, quartzite and sandstones. The sampling was performed with the aid of a water-cooled electric drill which incorporates a 2.5 cm-diameter diamond-coated bit. All samples were magnetically oriented with a magnetic compass and an inclinometer.

2.3. Laboratory procedures.

In the laboratory, samples were cut in order to obtain specimens with an approximate volume of 10 cm³. Some fragile samples were consolidated with a mixture of Sodium Silicate and water (75% and 25% respectively).

The natural remanent magnetization (NRM) stability was analysed by thermal (TH) and alternating field (AF) demagnetization of 36 representative specimens (from 36 different samples). TH demagnetization was carried out with a TD48-DC oven (ASC). It consisted of 19-23 demagnetization steps up to 650-675 °C. A 755 Superconducting Rock magnetometer (2G) was used to measure the remanence after each demagnetization step. In addition, one specimen from the brick fire tunnel and one specimen from the combustion chamber were demagnetized by alternate fields (AF) in 20 steps up to 100 mT. An automatic unit coupled to the magnetometer was used for this purpose. Software *Remasoft 3.0* (Chadima and Hroudá, 2006) was used to interpret the demagnetization data.

Low-field magnetic susceptibility (room temperature) was measured in all demagnetized specimens using a KLY-4 Kappabridge (AGICO). Königsberger ratio [$\text{NRM}/(\chi H)$, where χ is the magnetic susceptibility and H is the local magnetic field strength] (Stacey, 1967) was calculated. Anisotropy of the magnetic susceptibility (AMS) was measured in most of the demagnetized specimens (after the 200 °C step in those thermally demagnetized) and some additional non-demagnetized-specimens. Although the ideal would have been to measure it before starting the TH demagnetization, 200 °C is still a low temperature to modify

the magnetic properties, especially in burnt materials. AMS measurements were carried out with a KLY-4 Kappabridge, using the automated rotator system. AMS data were analyzed with the software *Anisoft 4.2* (Chadima and Jelinek, 2008).

Stepwise acquisition of isothermal remanent magnetization (IRM), hysteresis loops (± 1 T), backfield curves and thermomagnetic curves (temperature dependence of magnetization) were also carried out in some representative samples with a Magnetic Measurements' Variable Field Translation Balance (MM_VFTB). The results were interpreted with the software *RockMagAnalyzer* (Leonhardt, 2006). All the palaeomagnetic and rock-magnetic analyses were carried out in the Palaeomagnetism Laboratory of Burgos University (Spain).

3. RESULTS

3.1. Magnetic properties:

NRM values of specimens from the bricks of the fire tunnel vary between 6.4×10^{-2} and 8.8 A/m. Values from non-brick specimens range between 3.5×10^{-4} and 2.4×10^{-1} A/m. Initial magnetic susceptibility (room temperature) values are between 2×10^{-4} and 1.95×10^{-2} (dimensionless, SI) in the bricks and between 2.7×10^{-6} and 5.3×10^{-4} (dimensionless, SI) in the other materials. Königsberger ratio values are always above 1 and tend to be somewhat lower in non-brick specimens (values oscillate between 1.4 and 12.3) than in bricks (ranging between 1.8 and 23.5) (**Fig. 3**). Our Königsberger values are similar to those reported in analogous studies on kilns or other archaeological combustion structures pointing out that the magnetization is of thermal origin (i.e.: García Redondo et al. 2019; Carrancho et al. 2017).

Fig. 3. Königsberger ratio plot (white squares = bricks; black squares = other materials). Lines of constant Königsberger ratio (Q_n) between 0.1 and 100 are also shown.

Progressive acquisition of IRM shows the clear presence of high coercivity minerals in most bricks' samples (**Fig. 4a-e**). In non-brick samples, presence of high coercivity minerals is barely visible through the IRM curves (**Fig. 4g-i**). Thermomagnetic curves point to the common presence of magnetite in both materials (**Fig. 5**). A drop around 300 °C has been observed (e.g. **Fig. 5b**). It probably corresponds to the Curie temperature of highly substituted (Ti, Al, Mg) magnetite. Apart from magnetite, haematite is present in some samples according to the thermomagnetic curves: PW24A (**Fig. 5a**), PB1 (**Fig. 5g**) and PV1-1A (**Fig. 5h**) and less clearly, in PW32B (**Fig. 5c**) and PE4B (**Fig. 5e**). In some cases, a slight bump around 200 °C (followed by a drop around 250 °C) is observed in the heating curves (**Fig. 5d**). Epsilon iron oxide ($\epsilon\text{-Fe}_2\text{O}_3$) or low Curie temperature high coercivity stable phase (HCSLT) (López-Sánchez et al., 2017; McIntosh et al., 2007) has similar Curie temperatures. However, the inflexion around 250 °C should be also seen in the cooling curves, which is not the case. Bradák et al. (2020) detected a similar behaviour in Middle Palaeolithic combustion episodes and suggested that this could be an effect of the transition from SD to SP behaviour in magnetic grains close to the SSD/SP grain size boundary, as previously pointed out by Day (1975). All the thermomagnetic curves are highly reversible, with the only exception of a sample from the combustion chamber in which an important amount of secondary magnetite is formed (**Fig. 5h**).

Fig. 4. (a-i) Progressive acquisition of the Isothermal Remanent Magnetization (IRM) on representative brick samples (a-f; red triangles) and other materials (g-i; grey circles). [PE = samples from East Wall of the fire tunnel; PW = samples from the West Wall of the fire tunnel]

Fig. 5. (a-i) Thermomagnetic curves (temperature vs. magnetization) on (a-f) bricks' samples and (g-i) other materials corrected by paramagnetic fraction; (j-l) examples of hysteresis loops of bricks' samples (insets show the original cycles uncorrected by their dia-/paramagnetic fraction). [PE = samples from East Wall of the fire tunnel; PW = samples from the West Wall of the fire tunnel]

Anisotropy of magnetic susceptibility (AMS) results are summarized in **Table 1** and represented in **Fig. 6**. The average corrected anisotropy degree (P_j ; (Jelinek, 1981) of the bricks is 1.071, being $P_j < 1.040$ in most samples (29/49). Foliation predominates over lineation (**Table 1**), although there is certain variability in T values among specimens -especially in the West wall- (**Fig. 6a-b**). Minimum axis (k_3) is close to the vertical, indicating a horizontal foliation. Maximum axis (k_1) is parallel to the orientation of the walls (**Fig. 6a-b**). Non-brick specimens show average P_j values very scattered. Most of them are unreliable, since the mean susceptibility is low or very low and the number of measured specimens in this kind of materials is not usually high (**Table 1** and **Fig. 6h**). Orientation of the axes in these materials is variable depending on the area inside the combustion chamber. Predominance of lineation or foliation is also variable.

Table 1. AMS parameters (average values) with their respective standard deviation or 95 % confidence angles. (K_m = mean susceptibility; P_j = corrected anisotropy degree (Jelinek, 1981); T = averaged shape parameter (Jelinek, 1981); L = magnetic lineation; F = magnetic foliation.

Sampling area	N	K_m	St. Dev. (K_m)	P_j	St. Dev. (P_j)	T	St. Dev. (T)	L	St. Dev. (L)	F	St. Dev. (F)	$k1$			$k2$			$k3$					
												Dec. (°)	Conf. angle	Incl. (°)	Dec. (°)	Conf. angle	Incl. (°)	Dec. (°)	Conf. angle	Incl. (°)			
West wall (bricks)	26	6.0310 ⁻³	7.93110 ⁻³	1.0096	0.0083	0.0184	0.0416	1.0033	0.0031	1.0057	0.0077	354.3	48.9	17.2	23.5	88.2	48.9	12.4	22.3	21.4	24.4	68.6	21.6
East wall (bricks)	23	5.96110 ⁻³	8.39110 ⁻³	1.0042	0.0047	0.0181	0.0365	1.0006	0.0021	1.0024	0.009	326.9	20.6	4.2	18.1	23.3	8.8	19.1	8.2	3.3	3.3	80.3	15.9
PV 2	5	6.87	9.62	1.0085	0.0044	-0.051	0.081	1.0078	0.0074	1.0022	0.0089	109.5	45.3	36.2	20.8	31.9	50.1	31.3	7.1	4.1	4.5	38.4	28.1

Fig. 7a and c) is detected in most bricks and was isolated between 400/630 °C and 660/675 °C (only in one case up to 550 °C). That component is randomly oriented as can be observed in **Fig. 8b**. Exceptionally, some specimens exhibit a third component (Comp. I in **Fig. 7c)** between components A₁ and B. Components B and I are interpreted as records prior to the last heating of the structure (due to previous firings that reached higher temperatures and/or to the original component from the brick manufacture). In the case of the non-brick specimens, the component related to the last heating was isolated between 150/300 °C and 575/590 °C, showing normal polarity (Comp. A₂ in **Fig. 7d**).

Fig. 7. Representative examples of orthogonal NRM demagnetization diagrams and their respective normalized intensity plots. Solid/open circles in orthogonal plots represent the projections of vector endpoints onto the horizontal/vertical plane. [PE = samples from East Wall of the fire tunnel; PW = samples from the West Wall of the fire tunnel]. Specimen code, NRM intensity and type of material are also indicated.

Specimens exhibiting unstable demagnetization diagrams (i.e. **Fig. 7e)** and/or multicomponent diagrams with overlaps and anomalous directions (i.e. **Fig. 7f)** in which it was not possible to clearly identify and isolate the component related to last heating were excluded from the calculation of the mean direction. Most of them correspond to non-brick specimens (only 5 out of 19 non-brick specimens demagnetized were considered for the calculation of the mean direction). All directions of the components related to last heating (components A₁, A₂ and AF₁, shown in pink in **Fig.7)** along with the mean archaeomagnetic direction and associated statistical parameters according to Fisher (1953) are shown in **Fig. 8a**. The calculated mean direction for the western Vega's kiln is: declination (D) = 2.4°, inclination (I) = 62.2°, precision parameter (k) = 89.2, confidence angle (α_{95}) = 3.4°.

Fig. 8. Equal area projections of (a) record associated to the last heating and (b) component B directions together with the mean archaeomagnetic direction and associated statistical parameters. N is the number of specimens used to calculate the mean direction; N' is the total number of demagnetized specimens. k and α_{95} , precision parameter and confidence limit of the components related to last heating at the 95% level (after Fisher, 1953). [Solid/open symbols correspond to downward/upward inclination, respectively].

Archaeomagnetic dating was carried out with the Matlab tool designed by Pavón-Carrasco et al. (2011), using different geomagnetic models and the Iberian SV curve, relocated at the site coordinates. Based on the archaeological evidence available, our overall aim is to compare the dating results and evaluate their reproducibility. Five different geomagnetic records based on different input data, temporal and spatial coverage and modelling methods have been used to this goal. Firstly, two global models exclusively based on archaeomagnetic and lava flow data: SHA.DIF.14k (Pavón-Carrasco et al. 2014), spanning the last 14.000 years, and COV-ARCH (Hellio and Gillet, 2018), covering the last 3 millennia. Secondly, the global CALS3k.4 model (Korte et al. 2011), which ranges from 1000 BCE to 1900 AD and includes archaeomagnetic, lava flow and sedimentary data. Thirdly, the European model SCHA.DIF.4k (Pavón-Carrasco et al. 2021), based only on archaeomagnetic and lava flow data. Finally, the updated version of the Iberian secular variation curve ranging from 1000 BCE to 1900 AD and based on archaeomagnetic data was used (Molina-Cardín et al. 2018). Although the temporal coverage of these records is broad, particularly for SHA.DIF.14k, we have restricted it in all cases to 0-1900 AD for dating purposes. When SHA.DIF.14k model (Pavón-Carrasco et al., 2014) is used as reference, three different dating intervals at 95% of confidence are obtained: 0-64 AD, 455-691 AD and 1527-1649 AD (**Fig. 9a**). If model COV-ARCH is used, three possible dating intervals at 95% of confidence are obtained: 0-65 AD, 435-757 AD and 1530-1676 AD (**Fig. 9b**). In the case of CALS3k.4, four possible dating intervals at 95% of confidence are obtained: 0-126 AD, 369-551 AD, 573-590 AD and 1503-1637 AD (**Fig. 9b**). When using the regional model SCHA.DIF.4k, the possible dating intervals at 95% of confidence are also four: 0-50 AD, 450-653 AD, 662-749 AD and 1542-1674 AD. Finally, if the Iberian secular variation

curve is considered (Molina-Cardín et al., 2018), the dating intervals obtained at 95 % of confidence level are: 0-49 AD, 479-658 AD and 1556-1659 AD (**Fig. 9f**). The youngest dating intervals obtained with the different models/curve (1527-1649 AD by SHA.DIF.14k; 1530-1676 AD by COV-ARCH; 1503-1637 AD by CALS3k.4; 1542-1674 AD by SCHA.DIF.4K.1; and 1556-1659 AD by the Iberian SV curve) are the only coherent with the archaeological context.

Fig. 9. Probability-of-age density functions obtained with the tool from Pavón-Carrasco et al. (2011) for declination and inclination values using: (a) the SHA.DIF.14k model (Pavón-Carrasco et al. 2014); (b) the COV-ARCH model (Hellio and Gillet, 2018), (c) the CALS3k.4 model (Korte et al. 2011), (d) the SCHA.DIF.4k model (Pavón-Carrasco et. al., 2011) and (e) the Iberian SV curve of Molina-Cardín et al. (2018). Each panel shows the obtained declination (up, left) and inclination (up, right) represented together with the reference SV curve or model. The blue line represents the mean declination/inclination, and the green lines are their respective error bands at 95% confidence level. Just below them, it is shown the probability density function (PDF) for declination (left, down) and inclination (right, down). Finally, the combined PDF for both parameters is shown.

4. DISCUSSION

The palaeomagnetic and rock-magnetic results reported here depend on several factors, as the type of material studied, the samples' location in the kiln or the heating temperatures reached. In the following, the results will be discussed in terms of heat variability inside the kiln, the different types of materials analysed and their different history before they became part of the structure.

4.1. Heating temperatures

The combustion chamber most likely suffered the highest temperatures. However, the stability of the NRM seems to be higher in bricks than in the other materials. Unsuccessful directional record (i.e.: **Fig. 7e**) of most sandstones/limestones/quartzites (14 of them were

disregarded for the calculus of the mean archaeomagnetic direction) is interpreted as an effect of the low content of ferromagnetic minerals (*s.l.*) in these materials even after the heating. The lower values of magnetic susceptibility and NRM in the non-bricks materials than in the bricks (as it can be clearly seen in the Q_n plot: **Fig. 3**) point out in this direction. A possible explanation could be that the walls of the combustion chamber (where the sampled blocks come from) were plastered with a clay lining, which acted as a thermal insulator. Consequently, it would have affected to most samples from the chamber. This is rather common in archaeological pottery kilns to extend their use in time (i.e.: Broncano and Coll 1988; Yotov and Harizanov 2018) and it has been also observed in experimental archaeology reconstitutions (i.e.: Kassab Tezgör and Özsalar 2010). At the time of sampling such clay lining was absent, probably due to the progress of the excavation (part of the materials filling the combustion chamber were excavated) or a bad preservation.

As opposed to the quartzites, limestones or sandstones studied, bricks were exposed to high temperatures in their manufacture. The high reversibility in their thermomagnetic curves (**Fig. 5a-f**) is also a strong evidence of high-temperature heating (> 700 °C). As the kiln was used multiple times and probably at high temperatures, the ferromagnetic mineralogy is stabilized. That is, it does not transform when heated again in the lab up to 700 °C. Otherwise, heating and cooling cycles would clearly differ and that is not the case (**Fig. 5a-f**). Following the same reasoning, the low reversibility of the thermomagnetic curve of the sample PV1-1a (taken from the combustion chamber; **Fig. 5h**) is indicative that it did not reach a high temperature. This also agrees well with the aforementioned explained possibility of a clay-lining in the chamber. On the other hand, it is very interesting to analyze the directional NRM structure of bricks because it provides useful information not only for dating, but also to reconstruct the last firing record. This application has been occasionally explored in burnt archaeological materials of different age and nature (i.e.: Gose *et al.* 2000, Brown *et al.* 2009; Carrancho *et al.* 2016) and it can provide interesting technological information on the temperatures reached in a combustion structure. It is suggested that bricks of the fire tunnel reached relatively low

temperatures during their last heating (from 300 up to 610 °C according to the maximum unblocking temperatures -max T_{UB} - observed from the component related to the last heating of the kiln). Partial thermoremanence (pTRM) is interpreted as the main acquisition mechanism of the record associated to the last heating (Comp. A_1 in **Fig. 7a-c**). On the contrary, the direction of the high temperature component (Comp. B) in bricks is scattered (**Fig. 8b**). Our interpretation is that component B corresponds to the record acquired during the manufacture of the bricks, since their original position while baking is lost once they were placed in the kiln. The directional record shown by sample PW28-A (**Fig. 7c**) is particularly interesting as it provides additional evidence of multiple heating. The intermedium component I (from 475 °C to 610 °C) most likely corresponds to a heating after the manufacture heating (Comp. B) but before the last one in the kiln (Comp. A_1). The northward component A_1 is interpreted as a p-TRM and its maximal T_{UB} is 475 °C, which is interpreted as the temperature reached during last heating by this sample. A greater heating would have implied the resetting of components I and B. Considering that we are talking about the fire tunnel (the place through which fuel is introduced to feed the combustion chamber), it makes sense to observe pTRMs as **Fig. 7a and c** illustrates.

4.1. Mineralogical issues

It is worth mentioning some interesting behaviours of these materials from the mineralogical point of view. As far as the non-brick samples are concerned, magnetite is the main magnetic carrier. In burnt materials, it can be formed by the transformation of paramagnetic minerals (i.e.: phyllosilicates), or from the alteration of pre-existing Fe-bearing carbonates, sulphides or oxides with the necessary presence of organic matter (see i.e. Evans and Heller 2003 and references therein). Apart from magnetite, some contribution of hematite can be also distinguished from their thermomagnetic curves (**Fig. 5g-h**). Interestingly, that high-coercivity contribution is barely visible in their IRM acquisition curves (**Fig. 4g-i**). If the hematite grains contained in the non-brick samples were very fine-grained behaving as superparamagnetic (SP) grains (*s.s.*), they would not carry remanence (Dunlop and Özdemir 1997). That would explain why those SP hematite grains manifest primarily in the

thermomagnetic curves (induced magnetization) rather than in the IRM acquisition curves (only remanent magnetization). Anyway, the contribution to the magnetization of the high-coercivity fraction in the non-brick samples can be considered negligible. The occurrence of hematite is much more evident in bricks than in the other materials (see IRM curves in **Fig. 4a-f**). However, magnetite is the only mineral clearly recognizable in their corresponding thermomagnetic curves (**Fig. 5a-f**). The exceptions are sample PW24A (**Fig. 5a**) and to a lesser extent, samples PW32B and PE4B (**Fig. 5c and e**, respectively) with Curie temperatures slightly over 660°C indicating the coexistence of hematite. The wasp-waisted hysteresis loops of these samples (**Fig. 5j-l**), also suggest the coexistence of phases of different coercivities (Tauxe et al. 1996). The orthogonal NRM demagnetization plots along with their normalized decay intensity curves also indicate the contribution of hematite in the bricks' samples (**Fig. 7a-c**). Anyway, the directional record related to last heating presents intermediate maximum unblocking temperatures (475 °C in examples in **Fig. 7a and c**) and low coercivity (H_c) can be seen in the AF demagnetization of **Fig. 7b**) indicating that magnetite is the main carrier of the remanence.

4.3. Anisotropy of magnetic susceptibility

It is interesting to discuss the AMS results in bricks in relation with their manufacturing process. Maximum axis ($k1$) of the ellipsoid is on the horizontal plane, lined with the direction of the wall in which bricks are included (that is, parallel to the longest side of the bricks; **Fig. 6a-b**). The minimum axis ($k3$) is vertical. Hus et al. (2002) and Hus et al. (2003) described magnetic fabrics in bricks with the $k1$ coincident with the longest edges and the $k3$ perpendicular to the largest faces of the bricks. They linked this shape to the molding process during their manufacture. Thus, the observed fabric is probably related to the production of the bricks. According to Tema (2009), “the magnetic grains included in the clay mixture tend to be oriented parallel to the horizontal depositional” and “their long axes preferentially lie parallel to the brick's flat surface”.

It is worthwhile to discuss the AMS degree observed in the studied materials. In non-bricks materials, the results are questionable, since some areas present very low susceptibility values (i.e. PV2, **Table 1**; see also **Fig. 6h**). As shown in **Table 1**, the higher the susceptibility values, the lower the degree of anisotropy. Furthermore, the number of samples is usually low too. For these reasons, the values of anisotropy degree in non-brick materials are considered unreliable. In the case of the bricks, the higher values of susceptibility and the considerable number of measured specimens provide more reliable results. For AMS degree values between 1.053 and 1.074 (comparable to those reported here), Tema (2009) found values of Anisotropy of Isothermal Remanent Magnetization (AIRM) degree up to 1.753 and Anisotropy of Anhyseretic Remanent Magnetization (AARM) degrees up to 1.51. It implies an inclination shallowing from 4° to 10° for individual specimens. Similar values of inclination shallowing (from 2° to 13° at specimen level) were reported by Palencia-Ortás et al. (2017) in different types of combustion structures of Portugal. Declination is not usually severely affected (Tema, 2009, Palencia-Ortás et al. 2017). Kováčeva et al. (2009) evaluated the effect of the remanence anisotropy in the palaeointensity determinations through ATRM and AIRM experiments. They studied different non-ceramic archaeological materials (burnt soils, baked clay, bricks, tiles) and determined that the anisotropy correction in these materials (excluding pottery) was negligible in palaeointensity terms. In absence of further analyses of anisotropy of remanence here, we cannot totally exclude some bias in the directional results. However, some results suggest that it is highly unlikely. From a total of 21 specimens used for the mean direction calculation (we have AMS data from 19 of them), only 6 specimens (1 non-brick specimen and 5 brick specimens) present $P_j > 1.040$. The magnetic fabric of bricks is dominated by a horizontal foliation which could mainly affect the inclination. If we assume that non-brick specimens' anisotropy degrees are not reliable and we disregard the 5 brick specimens with $P_j > 1.040$ for the mean calculation, the inclination changes 0.3° (with respect to the obtained mean direction; **Fig. 8a**). Moreover, the k does not change much (from 89.2 to 85.0), indicating that distribution of the removed specimens is not so different from those preserved. If we remove the 6 specimens with $P_j > 1.040$ (including the non-brick one), the inclination changes only 0.2° (with

respect to the mean direction; **Fig. 8a**). Once again, k does not change significantly (84.1).

Therefore, it seems that the obtained directional mean value is not affected by anisotropy effects and can be considered as reliable. Apart from this, assuming a correction (increase) of a possible inclination shallowing and considering the constant increase of the inclination between 1350 and 1750 AD approximately, the resulting age would be younger than the most probable dating interval. As discussed below, in most cases, the most coherent dating interval was too young according to the documental evidences (which determine 1545 AD as the *terminus ante quem*; Archivo Municipal de Burgos, HI-3612).

4.4. Dating results

With respect to archaeomagnetic dating, several possible dating intervals at 95% of confidence level have been obtained using different geomagnetic records. The dating results are very similar regardless the reference model used. Considering the archaeological evidence available (i.e: stratigraphic data, typology of the pottery remains), in all the cases the youngest interval obtained (ranging between 1593 and 1676 AD) is the only coherent with the archaeological context. As opposed to magnetic inclination, the relatively slow variation in the declination of the Earth's magnetic field in Western Europe between *ca.* XIII-XVIIth centuries (see i.e. SCHA.DIF.4k model, Pavón Carrasco et al. 2021) results in a relatively wide probability density interval for this parameter. In spite of this, there is a good agreement between the probability density functions of declination and inclination, which is a further evidence of the reliability of the archaeomagnetic dating obtained.

The oldest age obtained for the last interval is more recent than the *terminus post quem* for the filling of the kiln after their last use (1469 AD) independently of the reference model/curve used. The youngest date is in all cases later than the *terminus ante quem* (1545 AD), reaching up to 1676 AD according to the COV-ARCH model. The resolution of the dating intervals is similar (122 years for SHA.DIF.14k, 146 years for COV-ARCH, 134 years for CALS3k.4, 132 years for SCHA.DIF.4K and 103 for the Iberian curve), corresponding the

shortest one to the Iberian Curve (**Fig. 9e**). It should be noted, however, that this interval obtained with the Iberian curve falls outside the expected archaeological age. The geomagnetic field models used probably have a higher data density than the Iberian curve and that explains the small temporal differences observed.

Nonetheless, although these temporal differences are small they may be relevant from the archaeological viewpoint. If we consider together the obtained results along with the archaeological and documental evidences, it would imply that the abandonment of the Western kiln of Vega's workshop took place between 1503 and 1545 AD. Assuming that the eastern kiln was closed after the western one, these results suggest that definitive abandonment of the workshop happened relatively close in time to the construction of the new houses in the place (at least, after 1503 AD). The obtained dating is in good agreement with the archaeological findings and supports the archaeological hypothesis that the studied Vega's kiln was intensively used for pottery production until the first half of the XVIth century AD. The archaeomagnetic dating provides the age of last use and potential abandonment of a combustion structure. This constitutes a considerable advantage over other dating methods such as radiocarbon, where the age can be determined by analyzing organic material associated with the structure but not necessarily as a result of its last use. This study is a nice testimony of how combining the archaeomagnetic dating (contrasted with various models) with archaeological information is necessary to constrain the last age of use as much as possible.

5. CONCLUSIONS

A pottery kiln from Burgos, north-central Spain, has been dated using a combination of archaeomagnetism and archaeological data. Unexpectedly, archaeomagnetic and rock-magnetic results show the suitability of bricks from the fire tunnel in contrast to the low intensity and less stable NRM behaviour of the materials from the combustion chamber (quartzites, limestones and sandstones). A clay lining over the chamber's materials probably limited the heat penetration there, resulting in an inefficient archaeomagnetic record. This demonstrates the

importance of sampling the entire structure since the combustion chamber does not necessarily provide the best archaeomagnetic results. Magnetite and variable contributions of hematite are the main ferromagnetic minerals identified. Moderately high AMS values have been observed in the bricks from the fire tunnel, but not high enough as to compromise the directional record. AMS data has revealed the manufacture fabric of bricks, which carry a stable characteristic remanent magnetization (mostly as a p-TRM) that allowed the determination of a well-defined archaeomagnetic direction. This direction was dated using four different geomagnetic models (SHA.DIF.14k, COV-ARCH, CALS3k.4 and SCHA.DIF.4k) and the Iberian SV curve. The resolution and the obtained datings is very similar regardless the model/curve used. Further refinement of the dating was suggested by combining with the archaeological information given by numismatic, stratigraphic and typological evidences resulting in an age of 1503 – 1545 AD. These results demonstrate the importance of sampling all the parts of a kiln, evaluating its anisotropy and other magnetic properties, using well-defined archaeomagnetic models for the period to be dated, and above all, close collaboration with archaeologists to refine the age of its last use.

ACKNOWLEDGEMENTS

Authors want to thank the comments of the editors and reviewers, who has contribute to improve the work. Special thanks are given to Sara Torres-López and Elisa M. Sánchez-Moreno for their collaboration during the sampling. We also want to thank Evaristo Giménez for facilitating the realization of the excavation. First author thanks the financial support of the European Social Fund (Operational Programme for Castilla y León) and the Junta de Castilla y León (Consejería de Educación). Authors also thank the support of the project CGL2016-77560-C2 financed by Spanish Ministry of Economy and Competitiveness (MINECO) and European Fund of Regional Development (EFRD), the project BU235P18 funded by Junta de Castilla y León and EFRD, and the projects PID2019-108753GB-C21 and PID2019-105796GB-I00 financed by Agencia Estatal de Investigación (Spain) [AEI /10.13039/501100011033].

FUNDING SOURCES

This work was supported by the predoctoral contracts' program co-financed by the European Social Fund (Operational Programme for Castilla y León) and the Junta de Castilla y León (Consejería de Educación), the project CGL2016-77560-C2 financed by Spanish Ministry of Economy and Competitiveness (MINECO) and European Fund of Regional Development (EFRD), the project BU235P18 funded by Junta de Castilla y León and EFRD, and the projects PID2019-108753GB-C21 and PID2019-105796GB-I00 financed by Agencia Estatal de Investigación (Spain) [AEI/10.13039/501100011033].

Author statement

Ángela Herrejón-Lagunilla: Conceptualization, Methodology, Formal Analysis, Investigation, Writing-Original Draft, Writing-Review & Editing.

Juan José Villalaín: Conceptualization, Methodology, Formal Analysis, Investigation, Writing-Original Draft, Writing-Review & Editing.

Ángel Carrancho: Conceptualization, Methodology, Formal Analysis, Investigation, Writing-Original Draft, Writing-Review & Editing.

Carmen Alonso-Fernández: Conceptualization, investigation, resources.

Javier Jiménez-Echevarría: Conceptualization, investigation, resources.

Declaration of interests

The authors declare that they have no known competing financial interests or personal relationships that could have appeared to influence the work reported in this paper.

The authors declare the following financial interests/personal relationships which may be considered as potential competing interests:

Supplementary data

Supplementary material 1

Supplementary material 2

REFERENCES

- Bradák, B., Carrancho, Á., Herrejón Lagunilla, Á., Villalaín, J.J., Monnier, G.F., Tostevin, G., Mallol, C., Pajović, G., Baković, M., Borovinić, N., 2020. Magnetic fabric and archaeomagnetic analyses of anthropogenic ash horizons in a cave sediment succession (Crvena Stijena site, Montenegro). *Geophys. J. Int.* 224, 795–812. doi:10.1093/gji/ggaa461
- Broncano, S., Coll, J., 1988. Horno de cerámica ibérica de La Casa Grande, Alcalá del Júcar (Albacete). *Noticiario Arqueológico Hispánico*, 30, 187-229.
- Brown, K.S., Marean, C.W., Herries, A.I.R., Jacobs, Z., Tricolo, C., Braun, D., Roberts, D.L., Meyer, M.C., Bernatchez, J., 2009. Fire as an engineering tool of early modern humans. *Science* 325, 859-862
- Carrancho, Á., Herrejón-Lagunilla, Á., Vergès, J.M., 2016. Three archaeomagnetic applications of archaeological interest to the study of burnt anthropogenic cave sediments. *Quaternary International* 414 (2016) 244-257
- Carrancho, Á., Goguita, A., Morales, J.I., Espinosa, J.A., Villalaín, J.J., Arsuaga, J.L., Baquedano, E., Pérez-González, A., 2017. Full-vector Archaeomagnetic dating of a medieval limekiln at Pinilla Del Valle site (Madrid, Spain). *Archaeometry* 59, 373–394.
- Chadima, M., Hroudá, F., 2006. Remasoft 3.0 – a user-friendly paleomagnetic data browser and analyzer. *Trav. Géophysiques XXVII*, 20–21.
- Chadima, M., Jelinek, V., 2008. Anisoft 4.2. - Anisotropy data browser, in: 11th Castle Meeting, Bojnice, Slovakia, 22–28 June.
- Crespo Redondo, J., 2007. La evolución del espacio urbano de Burgos durante la Edad Media. Editorial Dossoles, Burgos.

- Day, R., 1975. Some curious thermomagnetic curves and their interpretation. *Earth Planet. Sci. Lett.* 27, 95–100. doi:10.1016/0012-821X(75)90166-1
- Dunlop, D., Özdemir, Ö., 1997. *Rock Magnetism. Fundamentals and Frontiers*, Cambridge Univ. Press, New York
- Evans, M. E., Heller, F., 2003. *Environmental magnetism. Principles and Applications of Environmagnetics*. Academic Press. ISBN 9780122438516.
- Fisher, R., 1953. Dispersion on a sphere. *Proceedings of the Royal Society A. Mathematical, Physical and Engineering Sciences* 217, 295–305.
- Hellio, G., Gillet, N., 2018. Time-correlation-based regression of the geomagnetic field from archeological and sediment records. *Geophys. J. Int.* 214(3), 1585–1607.
doi:10.1093/GJI/GGY214
- García Redondo, N., Carrancho, Á., Gogutchichvili, A., Morales, J., & Palomino, Á., 2019. Comprehensive magnetic survey of kilns for bell and tile fabrication in Castile (Spain). *Journal of Archaeological Science: Reports*, 23(November 2018), 426–436.
doi:10.1016/j.jasrep.2018.11.003
- García-Redondo, N., Carrancho, Á., Gogutchichvili, A., Morales, J., Calvo-Rathert, M., Palomino, Á., 2020. New constraints on the medieval repopulation process in the northern Iberian plateau from the full vector archaeomagnetic dating of two hearths at La Pudia site (Caleruega, Burgos, Spain). *Archaeological and Anthropological Sciences* 12 (91).
doi:10.1007/s12520-020-01041-1
- Gose, W. A., 2000. Palaeomagnetic Studies of Burned Rocks. *Journal of Archaeological Science*, 27(5), 409–421. doi:10.1006/jasc.1999.0465
- Hus, J., Ech-Chakrouni, S., Jordanova, D., 2002. Origin of magnetic fabric in bricks: Its implications in archaeomagnetism. *Phys. Chem. Earth* 27, 1319–1331. doi:10.1016/S1474-7065(02)00126-2

- Hus, J., Ech-Chakrouni, S., Jordanova, D., Geeraerts, R., 2003. Archaeomagnetic investigation of two mediaeval brick constructions in North Belgium and the magnetic anisotropy of bricks. *Geoarchaeology* 18, 225–253. doi:10.1002/gea.10059
- Jelinek, V., 1981. Characterization of the magnetic fabric of rocks. *Tectonophysics* 79, 63–67. doi:10.1016/0040-1951(81)90110-4
- Kassab Tezgör, D., Özsalar, A. 2010. The reconstruction of a Roman Kiln in the Archaeological Museum of Sinop. *Ancient Civilizations from Scythia to Siberia* 16 (1-2), 199-216. doi: 10.1163/157005711X560381
- Korte, M., Constable, C., 2011. Improving geomagnetic field reconstructions for 0–3 ka. *Physics of the Earth and Planetary Interiors*, 188, 3-4, 247-259. <http://doi.org/10.1016/j.pepi.2011.06.017>
- Kovacheva, M., Chauvin, A., Jordanova, N., Manes, P., Karloukovski, V., 2009. Remanence anisotropy effect on the palaeointensity results obtained from various archaeological materials, excluding pottery. *Earth Planets Sp.* 61, 711–732.
- Leonhardt, R., 2006. Analyzing rock magnetic measurements: The RockMagAnalyzer 1.0 software. *Comput. Geosci.* 32, 1420–1431. doi:10.1016/j.cageo.2006.01.006
- López-Sánchez, J., McIntosh, G., Osete, M.L., del Campo, A., Villalaín, J.J., Kovacheva, M., Rodríguez de la Fuente, O., 2017. Epsilon iron oxide: Origin of the high coercivity stable low Curie temperature magnetic phase found in heated archeological materials. *Geochemistry, Geophys. Geosystems* 18, 2646–2656. doi:10.1002/2017GC006821
- McIntosh, G., Kovacheva, M., Catanzariti, G., Osete, M.L., Casas, L., 2007. Widespread occurrence of a novel high coercivity, thermally stable, low unblocking temperature magnetic phase in heated archeological material. *Geophys. Res. Lett.* 34, 1–5. doi:10.1029/2007GL031168
- Molina-Cardín, A., Campuzano, S. A., Osete, M. L., Rivero-Montero, M., Pavón-Carrasco, F.

- J., Palencia-Ortas, A., et al. 2018. Updated Iberian Archeomagnetic Catalogue: New Full Vector Paleosecular Variation Curve for the Last Three Millennia. *Geochemistry, Geophysics, Geosystems*, 19(10), 3637–3656. doi:10.1029/2018GC007781
- Palencia-Ortás, A., Osete, M. L., Campuzano, S. A., McIntosh, G., Larrazabal, J., Sastre, J., & Rodríguez-Aranda, J. (2017). New archaeomagnetic directions from Portugal and evolution of the geomagnetic field in Iberia from Late Bronze Age to Roman Times. *Physics of the Earth and Planetary Interiors*, 270, 183–194. doi:10.1016/j.pepi.2017.07.004
- Pavón-Carrasco, F. J., Campuzano, S. A., Rivero-Montero, M., Molina-Cardín, A., Gómez-Paccard, M., Osete, M. L., 2021. SCHA.DIF.4k: 4000 years of paleomagnetic reconstruction for Europe and its application for dating. *J. Geophys. Res. Solid Earth*, 1–18, e2020JB021237. doi:10.1029/2020JB021237
- Pavón-Carrasco, F.J., Osete, M.L., Torta, J.M., De Santis, A., 2014. A geomagnetic field model for the Holocene based on archaeomagnetic and lava flow data. *Earth Planet. Sci. Lett.* 388, 98–109. doi:10.1016/j.epsl.2013.11.046
- Pavón-Carrasco, F.J., Rodríguez-González, J., Osete, M.L., Torta, J.M., 2011. A Matlab tool for archaeomagnetic dating. *J. Archaeol. Sci.* 38, 408–419. doi:10.1016/j.jas.2010.09.021
- Stacey, F.D., 1967. The Koenigsberger ratio and the nature of thermoremanence in igneous rocks. *Earth Planet. Sci. Lett.* 2, 67–68. doi:10.1016/0012-821X(67)90174-4
- Tauxe, L., Mullender, T. A. T. & Pick, T., 1996. Pot-bellies, wasp-waists and superparamagnetism in magnetic hysteresis. *J. Geophys. Res.*, 101, 571–583
- Tema, E. (2009). Estimate of the magnetic anisotropy effect on the archaeomagnetic inclination of ancient bricks. *Physics of the Earth and Planetary Interiors*, 176(3–4), 213–223. doi:10.1016/j.pepi.2009.05.007
- Yotov, V., Harizanov, A., 2018. Ceramic Kilns in the Late Antique Town on Sveti Atanas Cape (Modern Day Byala, Bulgaria). *Pontica* 51.

Escritura de trueque y cambio entre la ciudad de Burgos y Juan Martínez de Lerma, por la que aquélla da a éste un poco de ejido entre su casa y su huerta del arrabal de Vega, a cambio de una tierra en el término de Castañares delante de un molino suyo llamado del Amor.

Archivo Municipal de Burgos, HI-3612

HIGHLIGHTS:

- An archaeomagnetic study of a kiln from the Vega's pottery workshop (Burgos, Spain) is reported here.
- Different materials (bricks vs. sandstones/limestones/quartzites) from distinct parts of the kiln (access corridor and chamber) have been sampled for their analysis.
- There is an important variability in the magnetic signature as a result of the thermal variation inside the structure, the composition of each material and its history before being part of the structure.
- Combination of archaeomagnetic, archaeological and documental evidences indicate that kiln's last usage took place during the first half of XVIth century AD (1503-1545 AD).

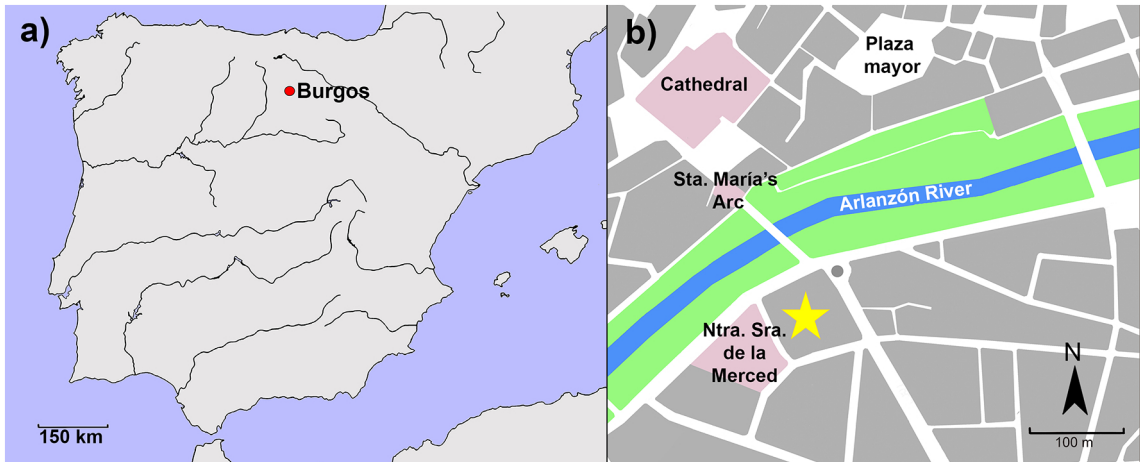


Figure 1

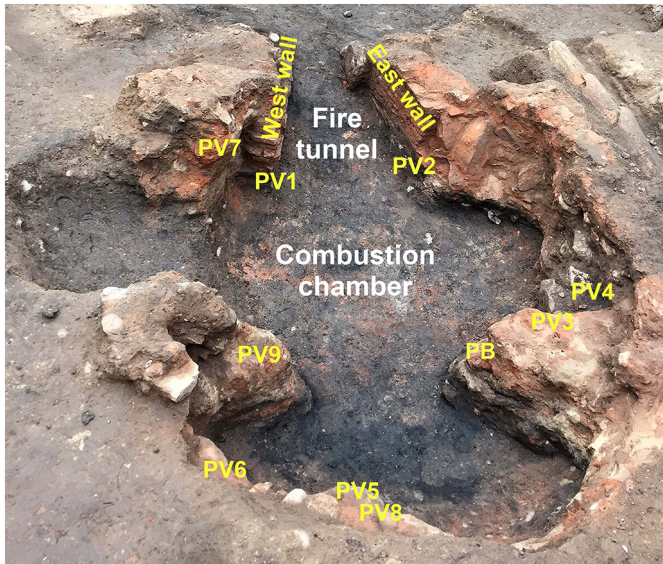


Figure 2

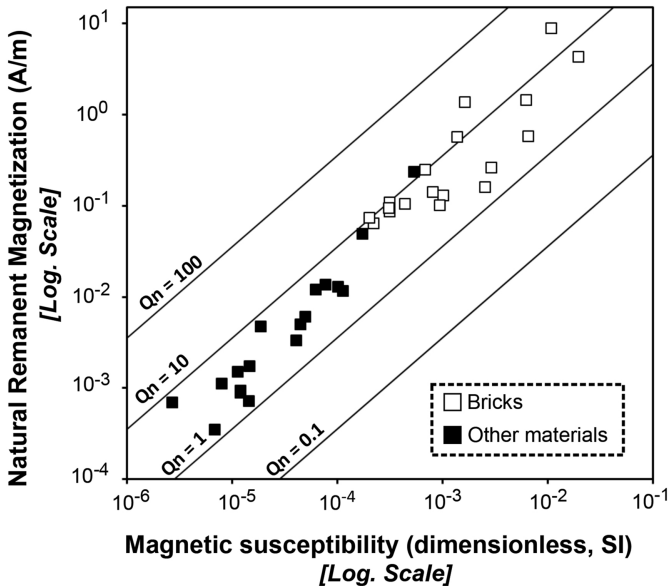


Figure 3

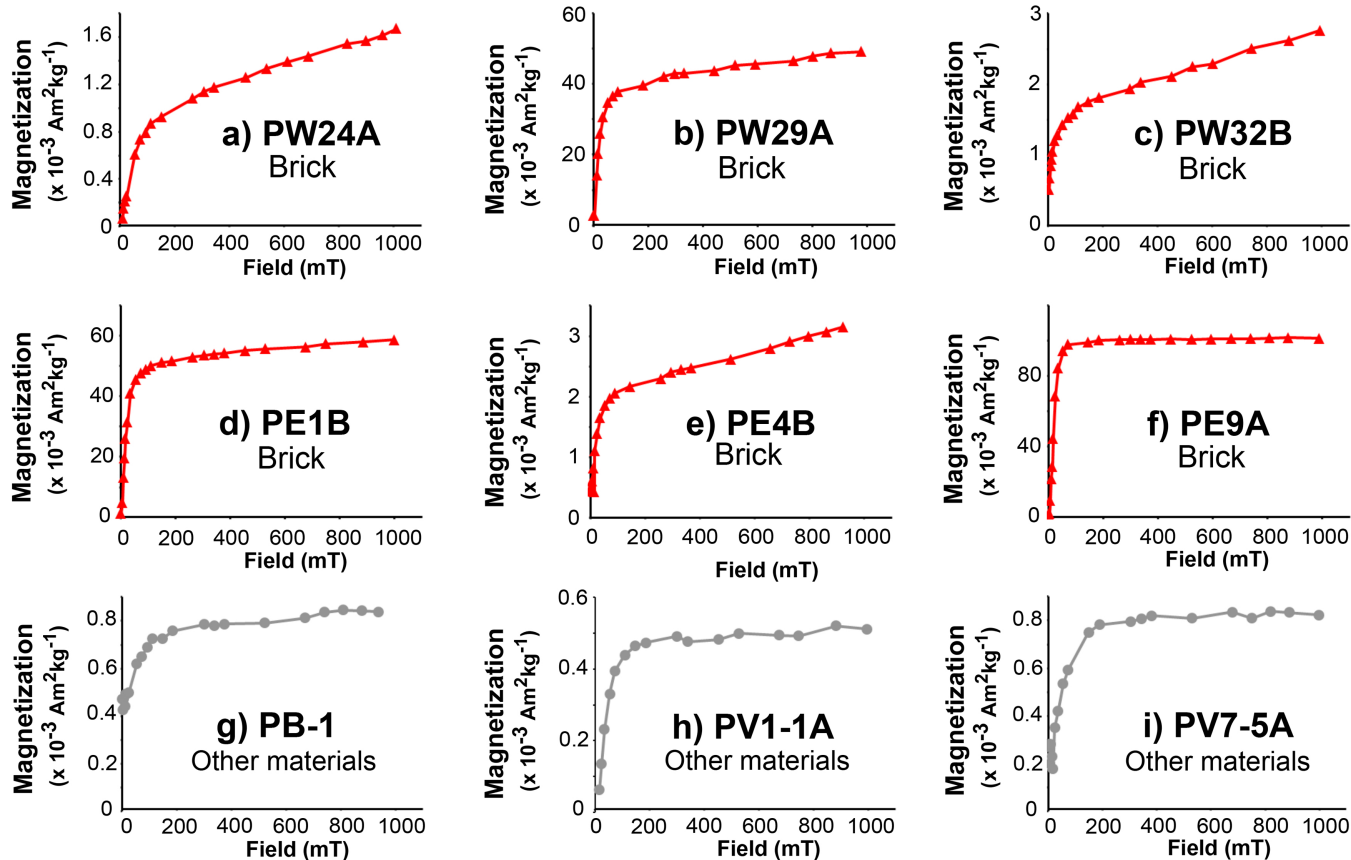


Figure 4

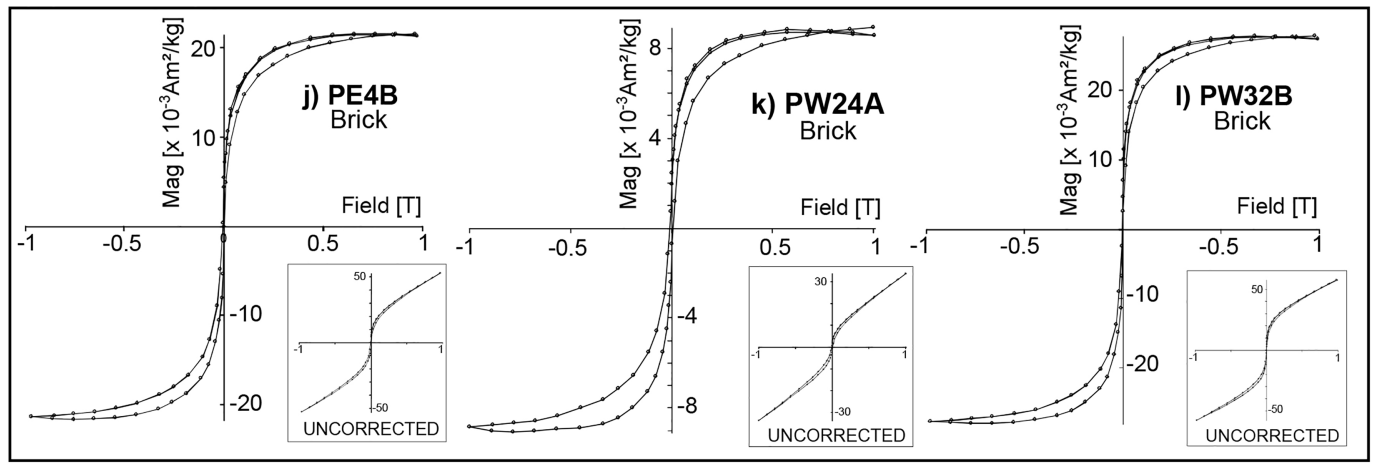
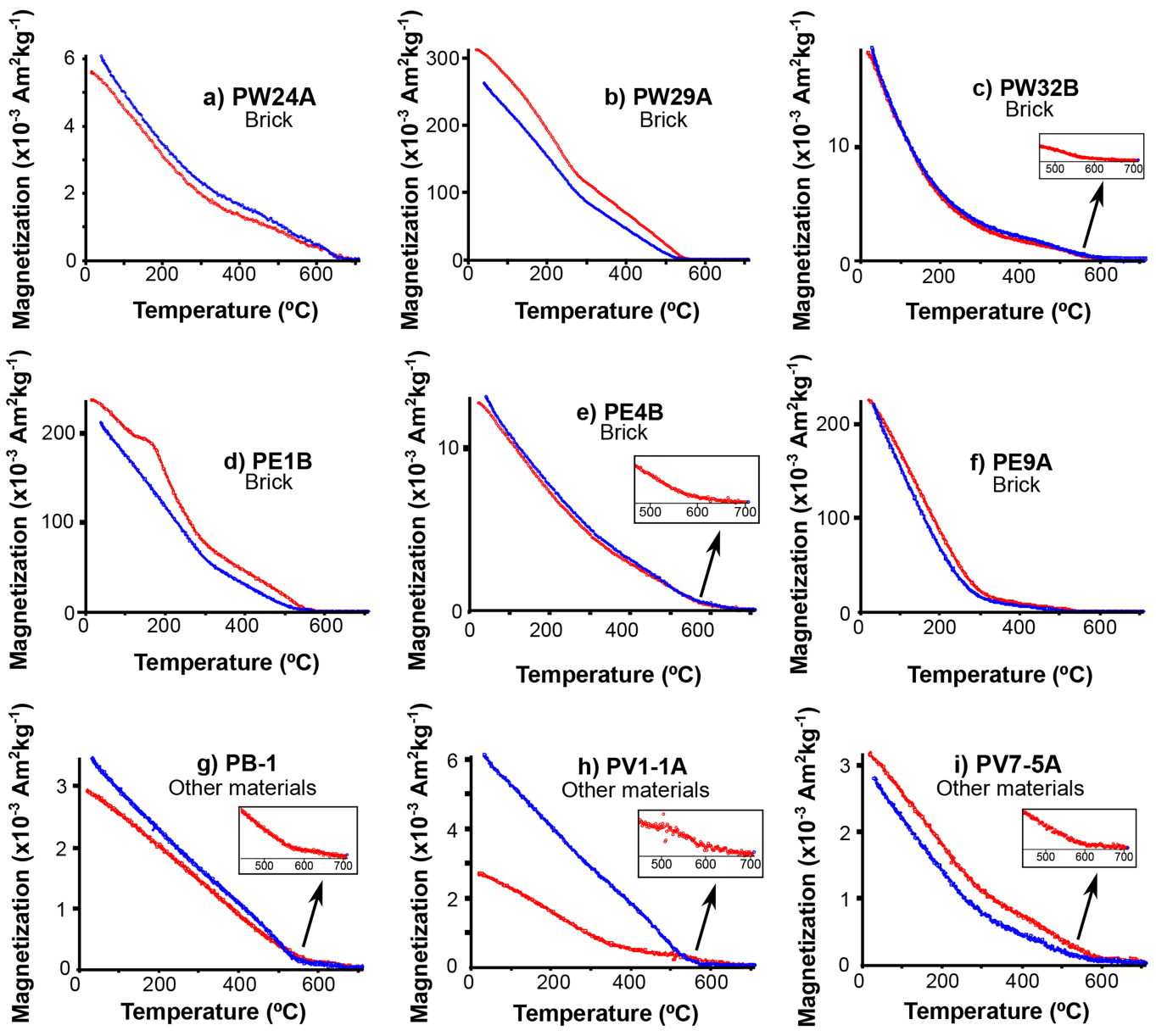


Figure 5

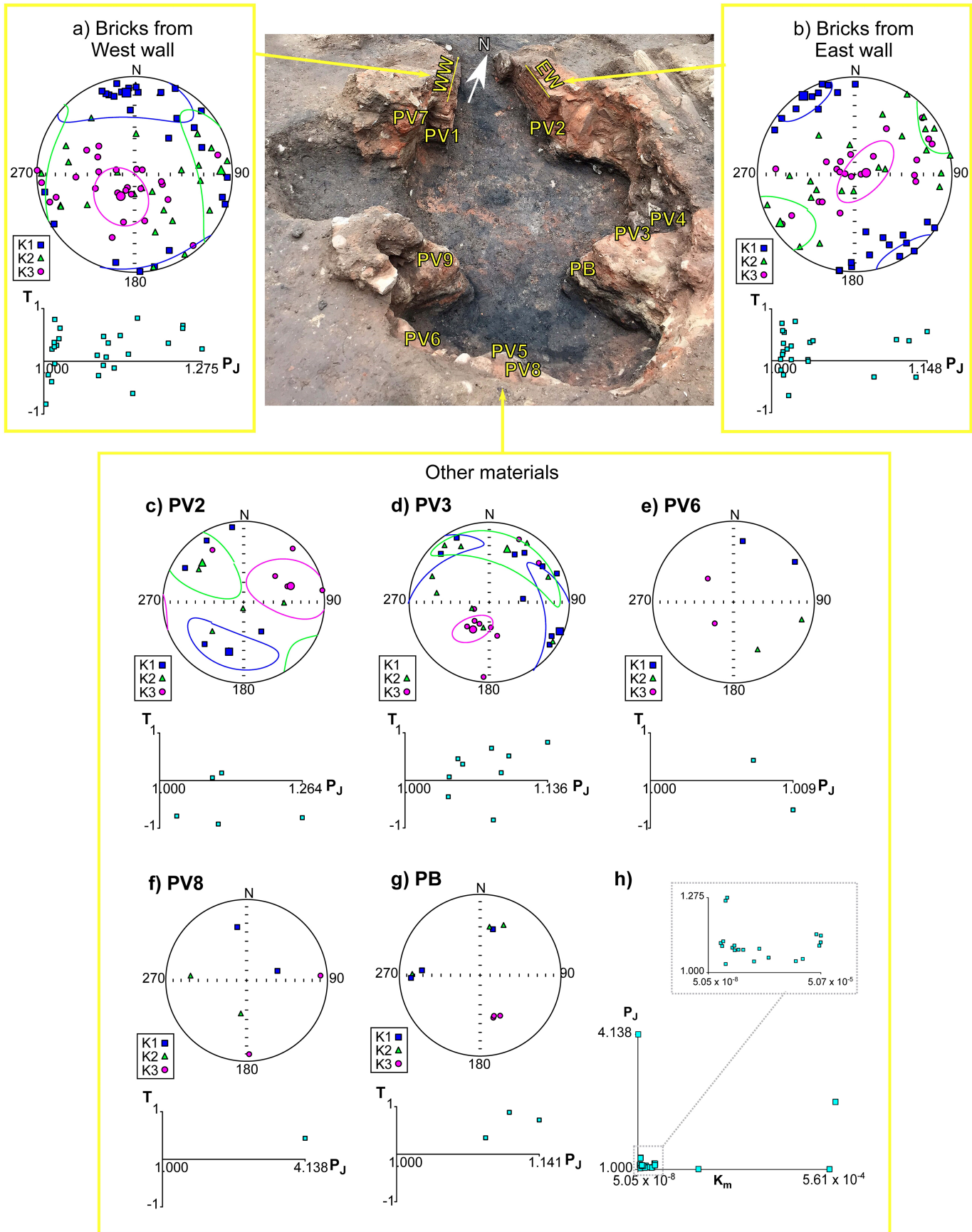


Figure 6

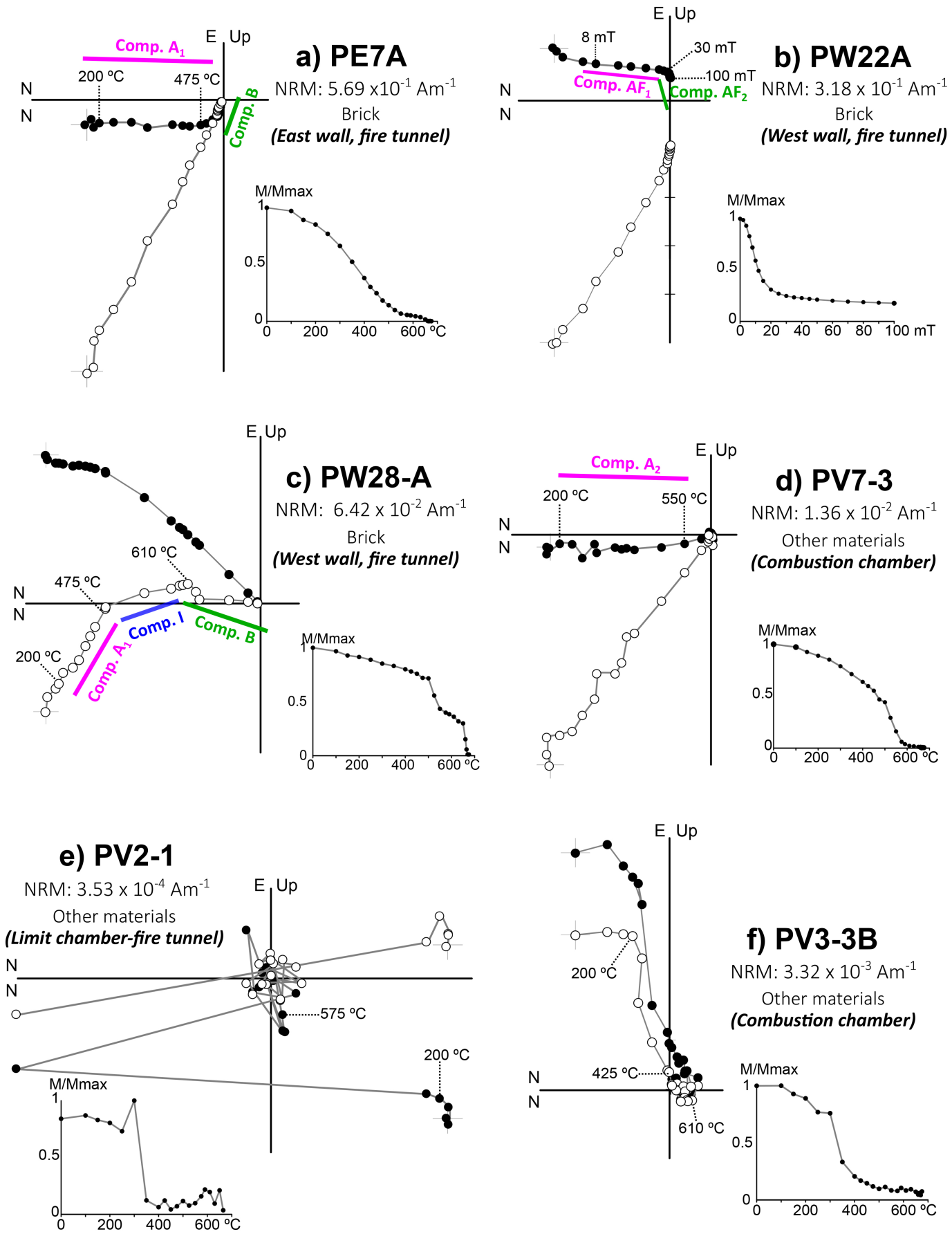
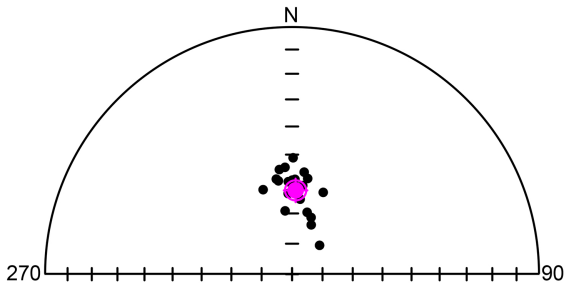


Figure 7

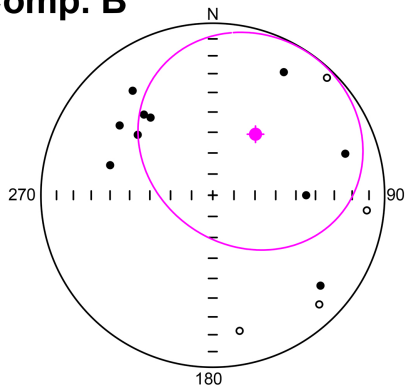
a) Record of the last heating

(Comp. A₁, Comp. A₂, Comp. AF₁)



N/N'	Dec. (°)	Inc. (°)	<i>k</i>	α_{95} (°)
21/38	2.4	62.2	89.2	3.4

b) Comp. B

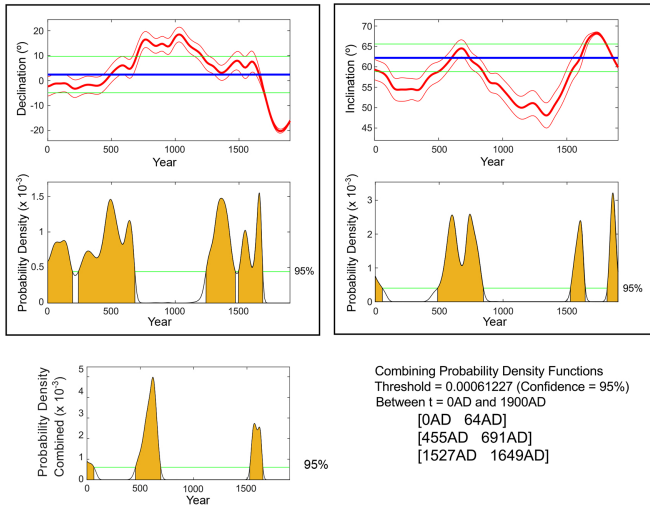


N	Dec. (°)	Inc. (°)	<i>k</i>	α_{95} (°)
14	35.0	54.3	1.5	54.0

Figure 8

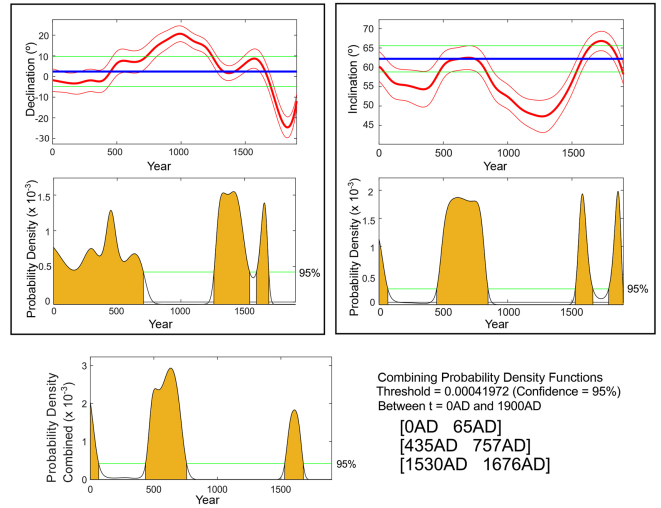
a) SHA.DIF.14k

(Pavón-Carrasco *et al.*, 2014)



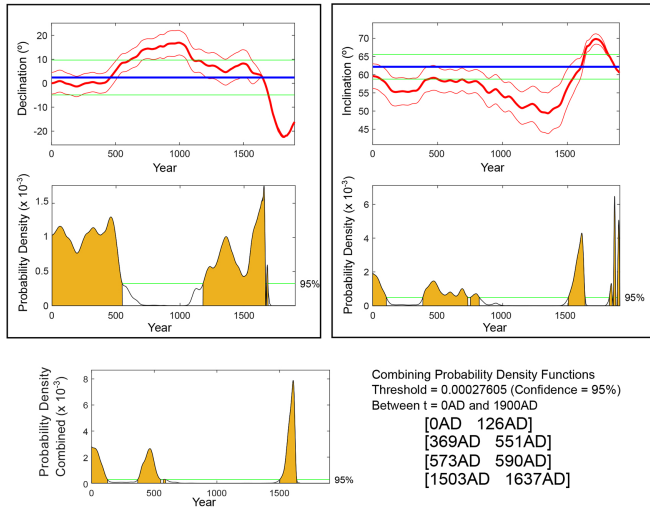
b) COV-ARCH

(Hellio and Gillet, 2018)



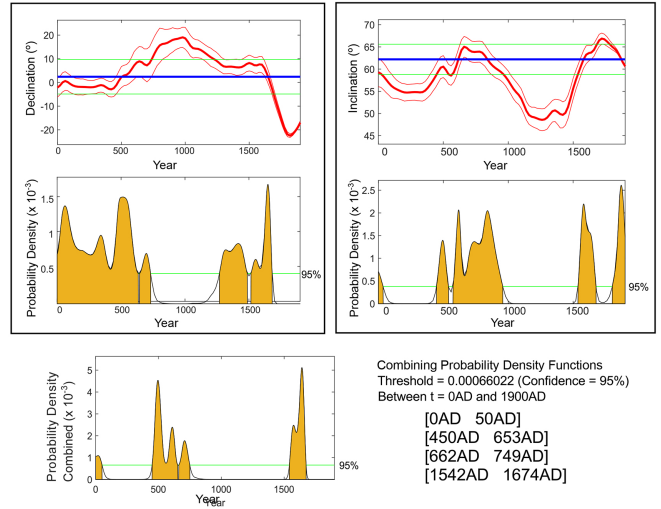
c) CALS3k.4

(Korte *et al.*, 2011)



d) SCHA.DIF.4K

(Pavón-Carrasco *et al.*, 2021)



e) Iberian SV Curve

(Molina-Cardin *et al.*, 2018)

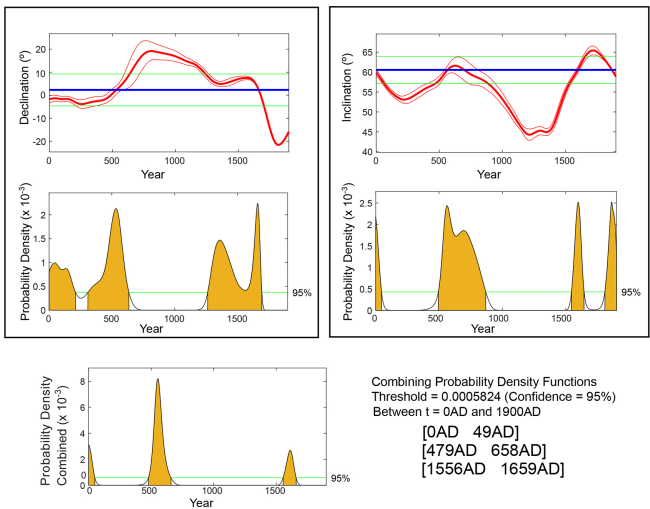


Figure 9